Int. J. Pharm. Investigation, 2024; 14(2):436-453.
https://www.jpionline.org

Original Article

Benzothiazolo-quinazoline Congeners Function as Anti-microtubule Agents Triggering Mitotic Arrest in Cancer Cells

Supriya Bhukya[1], Sonam Swain[1,4], Darna Mounika[3,4], Jyoti Honnanayakanavar[2,4], Battu Harish[2,4], Purna Chandra Behera[3,4], Vidya Jyothi Alli[3,4], Surender Singh Jadav[3,4], Anthony Addlagatta[1,4,*], Surisetti Suresh[2,4,*], Nishant Jain[1,4,*]

[1]Department of Applied Biology, CSIR-Indian Institute of Chemical Technology, Uppal Road, Hyderabad, Telangana, INDIA.
[2]Department of Organic Synthesis and Process Chemistry, CSIR-Indian Institute of Chemical Technology, Uppal Road, Hyderabad, Telangana, INDIA.
[3]Deptartment of Natural Products and Medicinal Chemistry, CSIR-Indian Institute of Chemical Technology Uppal Road, Tarnaka, Hyderabad, Telangana, INDIA.
[4]Academy of Scientific and Innovative Research (AcSIR), CSIR-HRDC Campus, Sector 19, Kamala Nehru Nagar, Ghaziabad, Uttar Pradesh, INDIA.

ABSTRACT

Background: Antimicrotubule agents effectively block cancer spread and are routinely employed as front-line chemotherapeutics. But patients, who receive Paclitaxel, suffer from peripheral neuropathy, which not only lowers quality of life but also can lead to treatment termination. Therefore, it is essential to identify novel microtubule inhibitors that can act as future front-line chemotherapeutics. In our previous study, we synthesized a cohort of 23 benzothiazolo[3,2-a] quinazoline derivatives employing a tandem copper catalyzed regioselective N-Arylation and aza-michael additions. However, the bioactive potential of the benzothiazolo-quinazoline derivatives are unknown. The synthesized benzothiazolo-quinazoline derivatives structurally resemble the microtubule inhibitors colchicine and CA-4. Therefore in this study; we asked whether benzothiazolo-quinazoline congeners act as microtubule inhibitors. **Materials and Methods:** To answer the question, we treated benzothiazolo-quinazoline congeners in a panel of four cancer cell lines and elucidated the molecular mechanism of action of the hit compounds *in vitro* and *in vivo*. **Results:** We found that benzothiazolo-quinazoline derivatives: 1-3, 6, 10, and 21-23 exhibited superior inhibitory effects with IC_{50} values ranging from 4.2-12.1 µM in HeLa cells. We observed that 1-3, 6, 10, and 21-23 arrest cells in G2/M phase and disrupt microtubule network. In addition, we found that the selected congeners increase transcript and protein levels of mitotic markers. As part of mechanism, we observed that the congeners 1-3, 6, 10, and 21-23 promote tubulin depolymerisation similar to nocodazole, a microtubule depolymerising agent. Further, molecular modelling studies have shown that the congeners occupy the colchicines binding pocket in microtubule. We observed that the congeners 1-3, 6, 10, and 21-23 disrupt blood vessel formation in chick eggs and arrest Zebrafish embryo development. **Conclusion:** We conclude that the congeners 1-3, 6, 10, and 21-23 function as antimicrotubule agents. Based on observations, we suggest that the congeners can be lead-optimized to generate next generation of frontline chemotherapeutics.

Keywords: Mitosis, Benzothiazolo-quinazoline, Molecular modelling, Tubulin, Zebrafish embryos.

Correspondence:
Dr. Surisetti Suresh
Department of Organic Synthesis and Process Chemistry, CSIR-Indian Institute of Chemical Technology, Uppal Road, Hyderabad-500007, Telangana, INDIA.
Email: surisetti@iict.res.in

Dr. Anthony Addlagatta
Department of Applied Biology, CSIR-Indian Institute of Chemical Technology, Uppal Road, Hyderabad-500007, Telangana, INDIA.
Email: anthony@csiriict.in

Dr. Nishant Jain
Department of Applied Biology, CSIR-Indian Institute of Chemical Technology, Uppal Road, Hyderabad-500007, Telangana, INDIA.
Email: nishant.iict@gov.in

Received: 12-09-2023;
Revised: 14-11-2023;
Accepted: 26-12-2023.

INTRODUCTION

Cancer is a malignancy that severely affects human health and well-being. Small molecules are routinely used as a treatment modality to ameliorate cancer and improve lifespan. The small molecules employed as anticancer agents belong into two categories that are molecules employed as front-line chemotherapy or molecules used as precision medicine. In most developing nations, front-line chemotherapy is a standard set for treating benign or advanced cancers, as it is relatively cost-effective.[1-4] In comparison, precision medicine, offers more targeted therapy with better outcomes and lesser side effects, but is cost-prohibitive.[1] Therefore, it is imperative to discover better front-line chemotherapy to ameliorate cancer. Among the front-line chemotherapy, the microtubule inhibitor Paclitaxel is administered to manage a wide range of cancers.[2] Paclitaxel binds to the taxol binding site in the α-Paclitaxel binds to the taxol

DOI: 10.5530/ijpi.14.2.54

binding site in the 5" thor><Year>2020</Year><RecNum>725</RecNum><DisplayText>.[2,3] The disruption in tubulin homeostasis triggers cell death termed as mitotic catastrophe.[4] However, Paclitaxel induces peripheral neuropathy as a side effect of chemotherapy.[5] In addition, 60-70% of patients who receive Paclitaxel suffer peripheral neuropathy, which not only lowers quality of life but also usually results in treatment termination.[6] Therefore, it is essential to identify novel microtubule inhibitors that can act as future front-line chemotherapeutics.

In our previous study, we synthesized a cohort of 23 benzothiazolo[3,2-a]quinazoline derivatives employing a tandem copper catalyzed regioselective N-Arylation and aza-Michael additions.[7] N-heterocycles have been extensively useful in a multitude of areas ranging from healthcare to energy.[8] Fused heterocycles such as benzothiazole[9] and quinazoline derivatives[10,11] have received much attention as these compounds have exhibited excellent biological activities. Benzothiazolo-quinazolines are a class of N-fused heterocycles, essentially constituted by the fusion of the benzothiazole and the quinazoline moieties. Linearly fused benzothiazolo-quinazolines such as benzothiazolo[2,3-*b*]quinazolinones have proved to display antitumor activities and acted as electrochemical sensors/biosensors[12-14] However, despite their interesting structures, the angularly fused benzothiazolo-quinazolines such as benzothiazolo[3,2-*a*]quinazolines have not been explored in the biological studies. Considering the importance of benzothiazoles and quinazolines as potential anti-cancer therapeutics,[9] we envisaged that the hybrid structures incorporating benzothiazoles and quinazolines moieties may have potential anticancer profiles. The angularly fused benzothiazolo-quinazoline derivatives 1-22 (Chart 1), incorporating a sp^3 carbon tethered with ester/cyano/alcohol group, were synthesized using tandem copper catalyzed N-arylation-aza-Michael addition from the coupling partners 2-aminobenzothiazole and *ortho*-halo cinnamic acid derivatives. The diaryl thioether 23, having cyanamido and acrylate functional groups, was an intermediate in the synthesis of benzothiazolo-quinazoline 2. The syntheses of compounds 1-23 and their structural analyses were reported in our previous study.[7] However, the bioactive potential of the benzothiazolo- quinazoline derivatives is unknown. Moreover, benzothiazolo-quinazoline derivatives structurally resemble the microtubule inhibitors colchicines and CA-4.[15,16] Therefore, in this present study, we asked whether benzothiazolo-quinazoline derivatives act as microtubule inhibitors. To answer the question, we treated benzothiazolo-quinazoline congeners in a panel of four cancer cell lines and elucidated the molecular mechanism of action of the hit compounds *in vitro* and *in vivo*.

EXPERIMENTAL PROCEDURES

Cell cultures, maintenance, and antiproliferative evaluation

The cell lines employed to determine IC_{50} values and perform molecular mechanism of action studies were obtained from ATCC. All the cell lines were grown in DMEM supplemented with 10% fetal bovine serum in carbon-dioxide incubator maintained at 37°C having 5 % CO_2. For determining IC_{50} values, we employed the NCI-60 study protocol. In brief, the benzothiazolo-quinazoline analogues were used in a 5-dose assay wherein the concentrations range from 0.01 M with a fold-increase to 100 µM. The compounds were diluted in DMSO, which also served as vehicle control in our assays. The cell lines were plated at 10,000 cells per well in a 96-well plate using the liquid handling system (Janus, Perkin Elmer) and grown overnight to confluency. Before treatments, for time zero, we performed SRB assay on a 96-well plate. The cells were treated with 5-doses of compounds for duration of 48 hr. After 48 hr, 0.1 mL of 10% TCA was added to the cells and 96-well plates were incubated on ice for 1.5 hr. Later, the medium containing 10% TCA was discarded and the bounds cells were washed 4 times with demineralised water and kept in a hot air oven for 1.5 hr. To check the amount of cells, we stained the 96-well plates using 0.6 % Sulforhodamine-B (SRB) obtained from (S4102, Sigma-Aldrich) for 30 min. After SRB staiing, the plates were kept in a hot air oven for 1.5 hr and then dissolved in 50 microliters of 10 mM Tris, pH:8 solution. The IC_{50} values were derived according to the NCI-60 protocol.[17]

Cell cycle distribution

HeLa cells were plated onto 60 mm dishes were treated with 1-3, 6, 10, 21-23 and nocodazole (M1404, Sigma) mitosis for 18 hr. Later the cells were washed three times using 1x PBS, trypsinized, and spun down at 1500 rpm for 10 min at 4°C. After centrifugation, the pellets were incubated in 950 microliters of 70% ethanol and incubated on ice for 2 hr. Subsequently, the cells were spun down at 1500 rpm at 4°C and the supernatants were discarded, after 2 times 1x PBS wash, the cell pellets were mixed with propidium iodide- RNAase solution made in 1x PBS. The flow cytometry was performed in Amnis Flowsight and histograms were plotted.[18]

Immunohistochemistry of tubulin and analysis of nuclear morphology

For immunohistochemistry analysis, HeLa cells were plated on 22 mm glass-coverslips and with 1-3, 6, 10, 21-23 and nocodazole for 18 hr. After incubation, the cells were fixed using 4% paraformaldehyde solution made in 1x PBS for 15 min at room temperature. Later the cells were washed three times using 1x PBS and subjected to permeabilization with 0.5% Triton X-100 and 0.05 % Tween-20 solutions made in 1xPBS for a duration of 6 min. Subsequently, the cells were blocked using 5% BSA made in 1x PBS for 2 hr. Primary antibody against tubulin (T6074, Sigma)

was used at 1:500 dilutions for primary staining. The cells were washed three times using 1x PBS and subjected to secondary antibody staining. Here, we used the Cy3 conjugated secondary antibody (AP124C, Sigma) at a dilution of 1:1000 for 2 hr. The cells were again subjected to 1x PBS wash and mounted onto slides using mounting media contacting DAPI (F6057, Sigma). The images of stained cells were captured with Nikon Eclipse Ti microscope.[19]

Western blot analysis of soluble versus polymerized tubulin

0.1 million HeLa cells were plated on 12-well plates overnight and treated with 1-3, 6, 10, 21-23, nocodazole or Paclitaxel (T7191, Sigma) for 18 hr. The cells were subjected to three times 1x PBS wash, and were ready to collect soluble and insoluble tubulin fractions. For soluble fractions, prewarmed lysis buffer was used as described previously. After incubation, the lysis buffer was aspirated and aliquoted into tubes containing 3x SDS-PAGE buffer. For insoluble fractions, we added 0.3 mL of 1 x SDS-PAGE to each well and harvested the samples. Both the soluble and insoluble fractions were heated in a boiling water bath for 5 mins. We loaded samples equally onto a 8% SDS-PAGE and subsequently transferred onto NC membranes using semi-dry transfer apparatus. 5% non-fat dry milk was added to the membranes and kept for 2 hr as blocking. Later, the membranes were incubated with tubulin antibody (T6074, Sigma) made in 1x TSBT at 1:2500 dilutions for 3 hr. The membranes were washed three times using 1x TBST and later incubated with 1:6000 dilutions of secondary antibody which was conjugated to HRP (A0545, Sigma) for 2 hr. The membranes were subjected to three washes and incubated with ECL solution and proteins were examined using ChemiDoc (LAS500, GE).[20,21] To determine Cyclin B1 (C8831, Sigma) and Aurora A (ZRB1902, Sigma) levels, HeLa cells treated with compounds were washed with 1x PBS, trypsinized, and subjected to Bradford assays. Equal amounts of protein were loaded onto SDS-PAGE gels and subjected to immunoblotting similar to the procedure followed to collect tubulin fractions.

Quantitative RT-PCR

HeLa cells were seeded on 10 cm dishes and treated with DMSO, 1-3, 6, 10, 21-23 and nocodazole for 18 hr. Subsequently, TRI reagent (T9424, Sigma) was used to isolate total RNA as per manufacturer's procedures. The total RNA was run on 1% agarose gel and RNA levels were quantified using NanoDrop 2000, Thermo. cDNA was made using superscript-III synthesis kit and the cDNA was aliquoted into 0.2 mL PCR tubes. Quantitative PCR was conducted in a PCR apparatus (CX96F, BioRad). The $\Delta\Delta C_t$ method was used to calculate fold change in mRNA levels and GAPDH was used for normalization.[22,23] Plk1 F: 5′-AAGAGATCCCGGAGGTCCTA-3', R: 5′-AAGAGATCCCGGAGGTCCTA-3'; Nek2A F: 5-'AATGAATCGCATGTCCTACAAT-3', R: 5'-CGTAATAATTTCATTCAATTCATCAG-3'; GAPDH F: 5' AACCTGCCAAGTACGATGACATC-3', R: 5'-GTAGCCCAGGATGCCCTTGA-3.'

ROS estimation

Compounds 1-3, 6, 10, 21-23 and nocodazole were used to treat HeLa cells which were plated onto 10 cm dishes. After treatments, the compound-treated cells were washed thrice with 1x PBS, trypsinized, and spun down for 2 min at 1500 rpm. The cell pellet were again washed and 20 µM DCF-DA (35845, Sigma) was added for 30 min in a CO_2 incubator maintained 37°C. After 30 min, the cells were washed using 1x PBS and fluorescence intensity was measured at λ_{ex}=485 nm/λ_{em}=520 nm in a Amnis Flowsight Flow cytometer and graph was plotted using Graph pad prism software.[18]

In silico molecular docking and ADMET

The protein tubulin-colchicine complex (PDB ID: 1SAO) was prepared and subjected to minimisation using "protein preparation" wizard from Schrodinger Suite using default parameters. For defining CBP using co-crystal colchicines, a receptor grid was constructed using "Receptor Grid Generation" wizard by taking default parameters and devoid of any constraints with a cube dimension of 25 Å. Simultaneously, the ligands were subjected to "ligprep" to generate possible ionized and minimized conformers employing default parameters. Subsequently the GLIDE software was employed, where the prepared ligands were docked into flexible SP (Standard Precision) and XP (Extra Precision) scoring functions taking the generated grid. Further, MM-GBSA (Molecular mechanics generalized Born surface area) studies were conducted to calculate the binding free energy of each protein complex using default parameters of PRIME module. The drug-like properties of these ligands were determined from data warrior and their respective toxicities were predicted using ProTox-II online server Schrödinger Release 2023-2: Maestro, Schrödinger, LLC, New York, NY, 2023.[24,25]

Annexin V-FITC

To detect for apoptosis, we employed the Annexin V methodology using the ApoAlert Apoptosis Detection Kit, Clontech. HeLa cells treated with indicated compounds were washed with 1x PBS and incubated with 10 µL of Annexin V-FITC and 10 µL of propidium iodide for 30 min. The stained cells were washed with 1x PBS and then mounted onto glass slides and images were captured using Nikon Ti Eclipse microscope.[17]

Measurement of Mitochondrial membrane potential using JC-1

The cationic dye JC-1 (T4069, Sigma) was used to determine mitochondrial membrane potential ($\Delta\Psi m$). In the mitochondria of healthy cells, JC-1 accumulates and exhibits red fluorescence and when mitochondria are depolarised, JC-1 uptake is restricted

Table 1: Anti-cancer activity of the compounds 1-23 IC_{50} values are listed.

Compound ID	Compound Structure	HeLa	MDA-MB-231	PC3	DU145
1	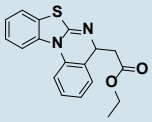	4.23± 0.25	5.36±1.2	6.81±1.21	10.15±2.56
2	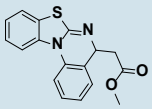	4.75±0.36	5.91±0.86	5.78±1.48	11.56±1.52
3	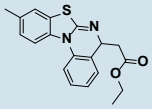	5.01±1.12	6.58±1.56	9.76±1.63	12.14±1.45
4	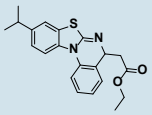	27.85±3.4	28.96±4.01	18.96±2.15	35.69±1.54
5	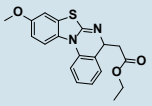	22.63±2.52	24.87±1.89	25.34±2.36	34.52±3.52
6	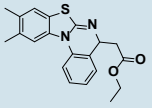	5.51±0.79	5.74±0.95	7.56±1.25	11.54±1.54
7	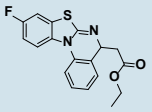	24.86±2.65	22.58±1.99	36.84±5.41	45.17±2.69
8	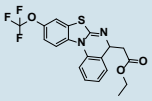	36.11±1.25	28.12±5.63	50.25±7.12	96.32±8.52
9	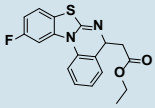	27.86±2.56	41.75±3.36	18.23±1.23	29.54±5.23
10	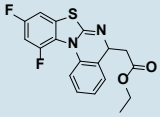	8.12±1.12	9.25±1.35	10.52±2.13	18.23±1.79
11	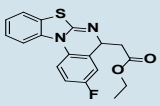	19.56±1.52	25.62±4.56	38.96±4.12	59.65±5.36
12	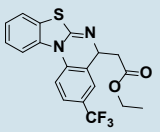	27.55±1.54	36.52±2.35	27.56±3.65	48.91±3.65
13	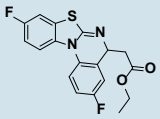	26.58±2.36	35.25±8.32	87.63±11.23	65.41±5.87

Compound ID	Compound Structure	HeLa	MDA-MB-231	PC3	DU145
14	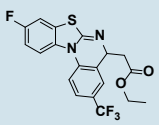	26.84±3.69	37.23±3.65	35.12±4.63	68.11±4.65
15	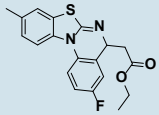	35.24±2.36	27.12±1.75	56.58±9.84	47.15±4.52
16	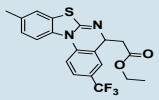	33.58±3.54	35.63±6.48	18.14±1.29	65.23±5.36
17	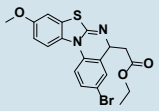	22.54±1.12	45.65±2.85	36.78±4.21	54.35±7.86
18	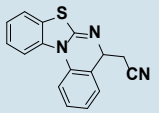	26.69±1.75	41.25±1.25	36.89±4.56	78.56±12.56
19	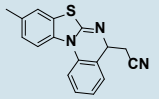	31.25±1.36	30.56±2.69	58.96±7.96	45.63±8.12
20	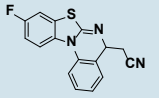	18.89±1.15	19.38±1.75	20.77±1.45	63.89±6.45
21	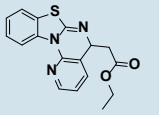	8.85±1.65	9.77±1.36	11.23±2.56	15.65±1.42
22	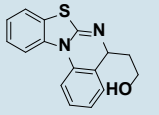	10.12±1.63	14.56±2.10	17.81±1.63	23.56±1.45
23	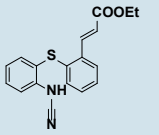	9.35±1.70	9.89±1.14	10.11±1.25	12.41±1.25
24	Nocodazole	1.2±0.8	1.7±0.5	2.1±0.85	2.2±0.75

and shows green fluorescence. To perform JC-1 assays, HeLa plated on coverslips treated with compounds were washed using1x PBS and stained employing 5 µg/mL JC-1 dyes. The stained cells were incubated at room temperature in dark for 30 min and later washed using 1x PBS and mounted on coverlips for confocal imaging (Nikon Ti Eclipse).[17]

Chick embryo angiogenesis assay

The assay is extensively employed in diverse applications in biology to investigate alterations in blood vessel creation throughout a chick's developmental stages. Fertile chicken eggs were obtained from the ICAR-Directorate of Poultry Research, Rajendranagar, Hyderabad, India, in order to conduct the assay. The viable eggs were cultured at 37°C with 60-70% relative humidity. On the air sack side, a tiny opening was created on the fourth day of incubation. After the top of the shell was carefully cracked off, the chosen chemicals were applied. Additionally, the eggs were incubated in the incubator for an additional 4 hr following treatments. Stereomicroscope (S8APO, Leica) photographs of the

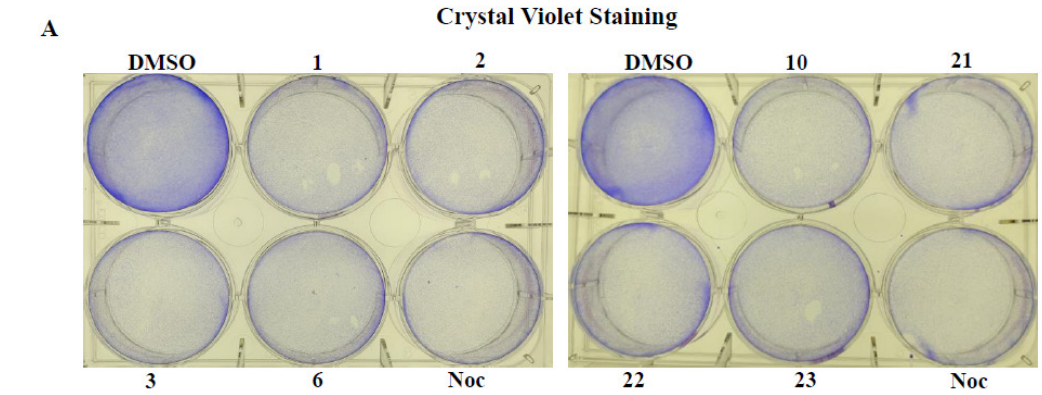

Compounds	DMSO	Noc	1	2	3	6	10	21	22	23
% of Growth Inhibition	5	94	95	92	86	71	75	72	67	62

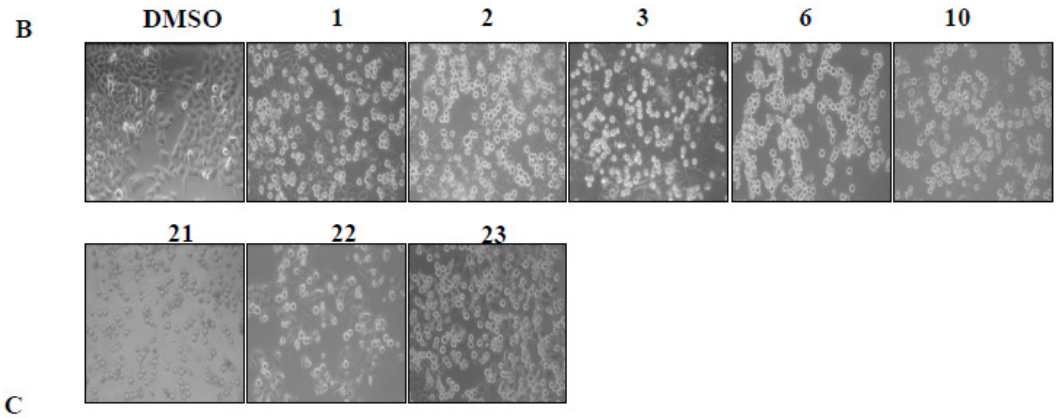

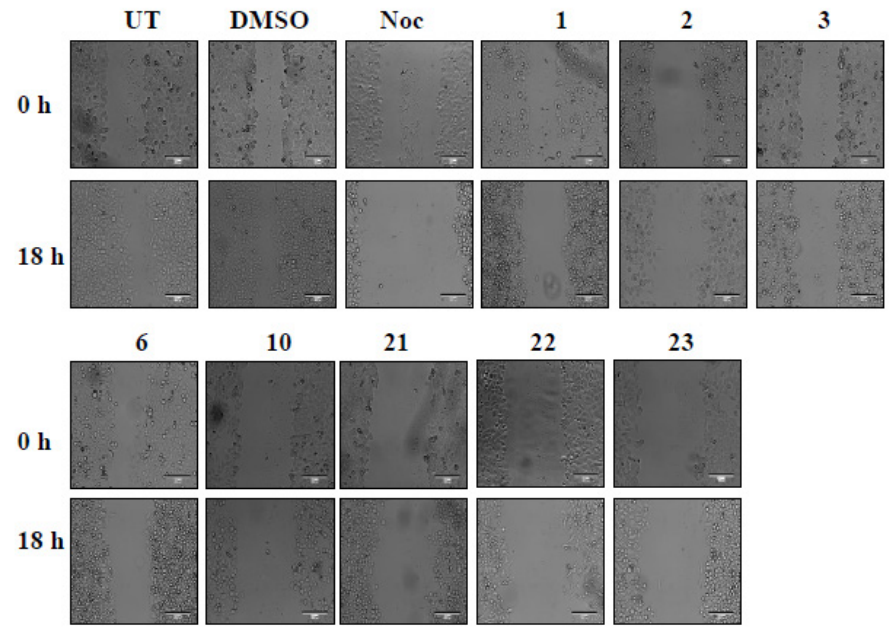

Figure 1: Benzothiazolo-quinazoline congeners 1-3, 6, 10, and 21-23 reduce HeLa cell growth-A, HeLa cells seeded on six-well plates were treated with 5 µM of 1-3, 6, 10, and with 10 µM 21-23 for 18 hr. Nocodazole (Noc) was used as a positive control, at 2.5 µM concentrations After 18 hr, cells were washed with 1x PBS, stained with crystal violet dye, and cell density was determined. The images are representative of three independent experiments. B, HeLa cells seeded on six-well plates were treated with 5 µM of 1-3, 6, 10, and with 10 µM of 21-23 for 18 hr. Images of cells were captured using phase-contrast microscopy, *n*=3. C, HeLa cells seeded on six-well plates overnight were scratched using a pipette tip and photographed. After capturing images at 0 hr, the cells were treated with 5 µM of 1-3, 6, 10, and with 10 µM 21-23 for 18 hr. The images were captured using phase-contrast microscopy, *n*=3.

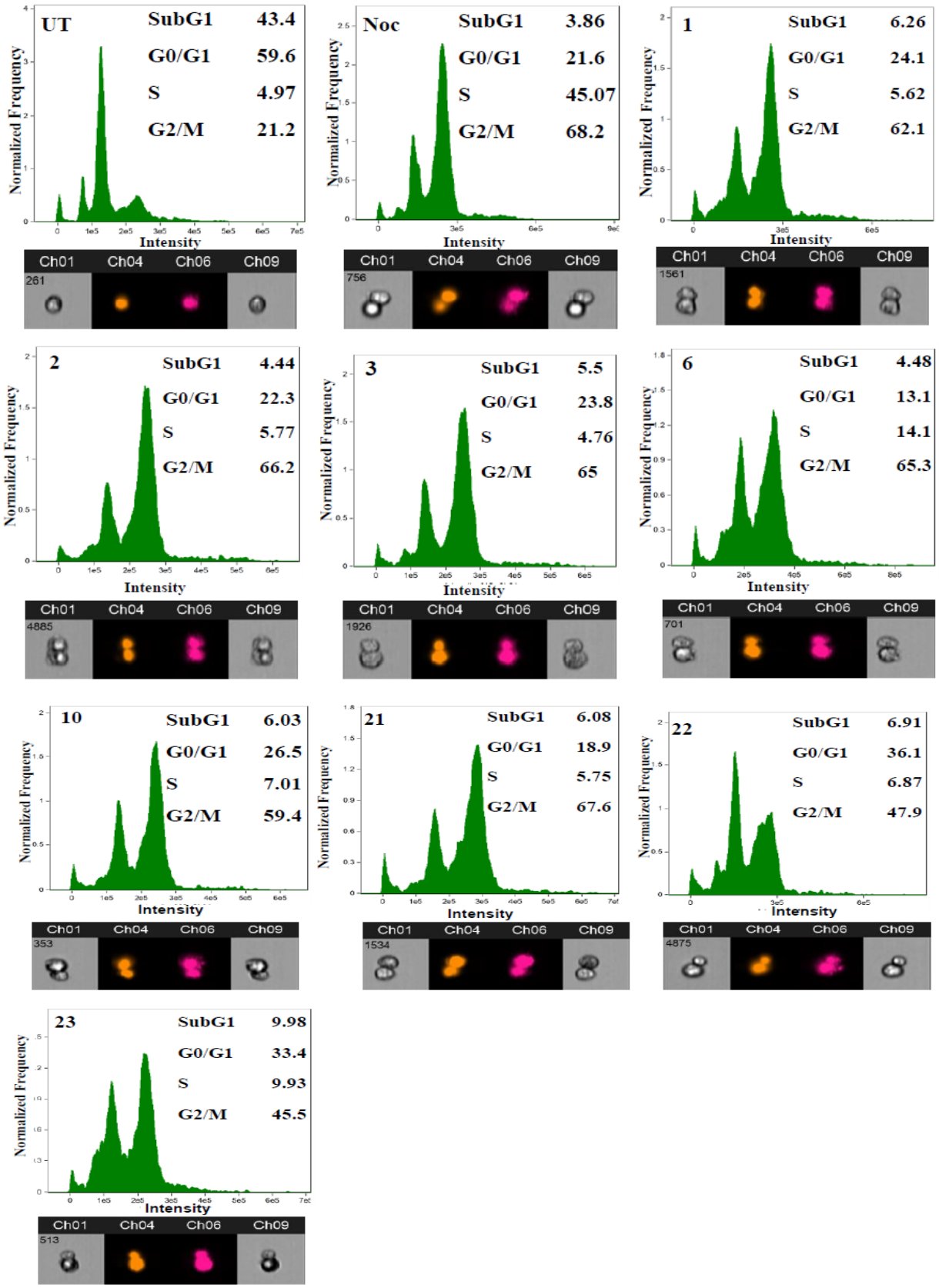

Figure 2: Benzothiazolo-quinazoline congeners 1-3, 6, 10, and 21-23 trigger G2/M or mitotic arrest- A, HeLa cells seeded onto 60 mm dishes were treated with 5 µM of 1-3, 6, 10, and with 10 µM 21-23 for 18 hr. Nocodazole (Noc) was used as a positive control, at 2.5 µM concentrations After 18 hr, cells were washed with 1x PBS, fixed with 70% ethanol, stained with propidium iodide and cell cycle was determined using flow cytometry. The images are representative of three independent experiments. Representative images of captured cells are highlighted with each of the histogram, *n*=3.

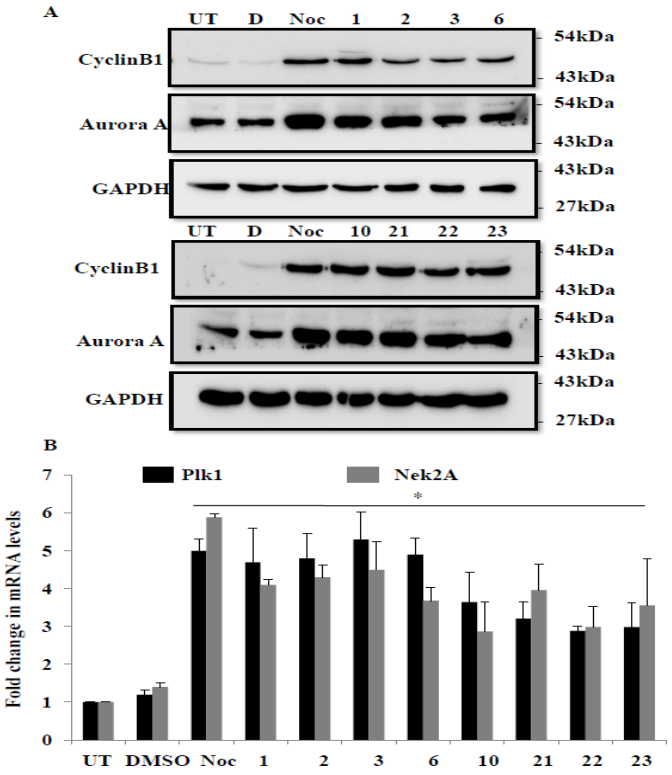

Figure 3: Benzothiazolo-quinazoline congeners induce accumulation of protein and transcripts of mitotic markers-A, HeLa cells seeded onto 60 mm dishes were treated with 5 µM of 1-3, 6, 10, and with 10 µM 21-23 for 18 hr. Nocodazole (Noc) was used as a positive control, at 2.5 µM concentrations. After 18 hr, cells were washed with 1x PBS, lysed using 1x RIPA buffer, and quantified with Bradford assays. Equal amounts of protein were resolved in 10% SDS-PAGE, and the protein levels of Cyclin B1 and Aurora A were detected using specific antibodies. GAPDH was used as normalization control. The images are representative of three independent experiments. B, under similar treatment conditions as A, the mRNA levels of Plk1 and Nek2A were analyzed by qPCR. After normalization to GAPDH, the gene expressions were represented as normalized mRNA fold change (mean±SD), *p<0.05, and n=3.

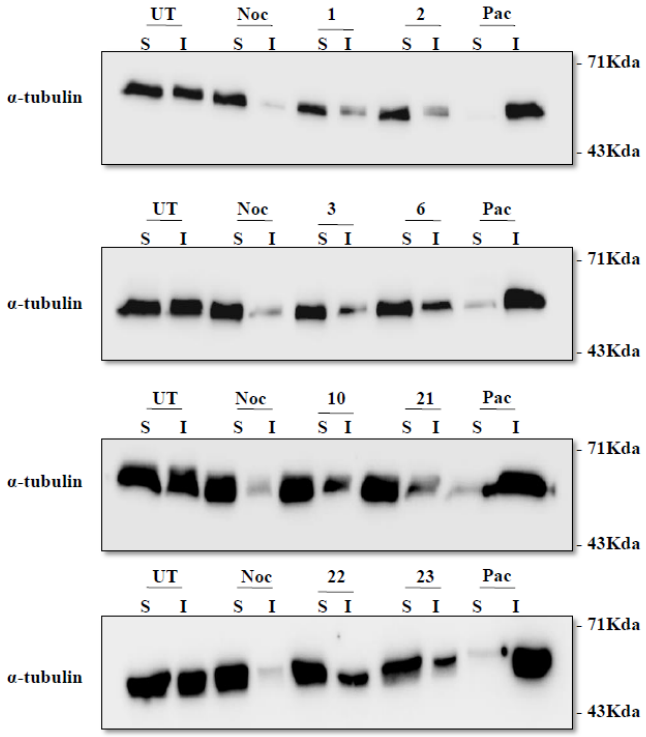

Figure 4: Benzothiazolo-quinazoline congeners act as microtubule depolymerising agents- HeLa cells were plated onto 12-well plates and treated with 5 µM of 1-3, 6, 10, and with 10 µM 21-23 for 18 hr. Nocodazole (Noc) was used at 2.5 µM concentrations and Paclitaxel (Pac) as at 1 µM concentrations for 18 hr. The distribution of tubulin in solublevs. insoluble fractions as analyzed by immunoblotting. The fractions containing soluble and polymerised tubulin were collected and separated by SDS-PAGE. Tubulin was detected by immunoblot analysis, n=3.

treated and untreated eggs were taken at 0 and 4 hr, respectively. The ImageJ program was used to quantify the blood vessels.[26,27]

Zebrafish screening

Wild type zebrafish (*Danio rerio*) were bred and kept under conditions of 28.5°C with 14 h:10 hr light-dark cycles. Three pairs of zebrafish mated simultaneously, and the resulting embryos were combined. After dechlorination, three to four embryos were placed in each well of a 48-well plate using 0.4 mL of E3 embryo medium. The embryos were incubated at 28.5°C after being treated with specific drugs at 10 µM and 20 µM, nocodazole at 2.5 µM and 5 µM, or DMSO (1%) at 5 hr after fertilization. In biological replicates, roughly 6-7 embryos were examined for every chemical. They were examined using bright-field microscopy (Olympus, IX73) 28 hr after conception. Only substances that produced comparable phenotypic abnormalities in the majority of the embryos were regarded as active.[28,29]

Statistical analysis

The student's t-test was used to calculate statistical differences. Using a two-tailed t-test, p values for pair-wise comparisons were deduced, p<0.05 was considered significant.

RESULTS

Structure-activity Relationship of benzothiazolo-quinazoline congeners

In this study, *in vitro* inhibition of the benzothiazolo-quinazoline derivatives 1-22 and diaryl thioether 23 were tested towards HeLa, MDA-MB-231, PC3 and DU145 cell lines. The IC_{50} values are summarized in Table 1. The methyl 2-(5H-benzo[4,5]thiazolo[3,2-a]quinazolin-5-yl)acetate 1 exhibited excellent inhibition with IC_{50} values of 4.2 µM, 5.4 µM, 6.8 µM and 10.5 µM towards HeLa, MDA-MB-231, PC3 and DU145 cell lines, respectively. Similarly, 2-(5H-benzo [4, 5]thiazolo[3,2-a]quinazolin-5-yl)acetates 2 and 3 exhibited

excellent inhibition of HeLa, MDA-MB-231, PC3 and DU145 in the range of 4.7-12.1 μM (IC_{50}). It may be noted that the compounds 1-3 showed similar inhibitory effects across the four cell lines. However, benzothiazolo-quinazolines 4 and 5, containing isopropyl and methoxy substituents on the benzene ring of the benzothiazole moiety, exhibited inferior inhibitory effects. It must be noted that benzothiazolo-quinazoline 6, having two methyl substituents performed well with IC_{50} values of 5.5-11.5 μM, which are similar to the compounds 1-3. Benzothiazolo-quinazolines 7-9, bearing electron withdrawing groups (F, OCF_3) provided weak inhibition towards the four cell lines. Interestingly, benzothiazolo-quinazoline 10, with two fluorine groups on the benzene ring of the benzothiazole moiety displayed superior pan-inhibitory effects with IC_{50} values ranging from 8.1-18.2 μM. Compounds having electron withdrawing groups (F, CF_3) on the benzene ring of the quinazoline moiety such as 11 and 12 returned much lower IC_{50} values. Benzothiazolo-quinazolines 13-17, bearing substituent's on both the benzene rings of the benzothiazole and quinazoline moieties, also exhibited lower inhibition across the four cell lines. In the place of the ester group of the benzothiazolo-quinazoline, we employed a cyano group. Accordingly, cyano tethered benzothiazolo-quinazolines 18-20 were examined to observe low inhibitory activities. Note that N-doped benzothiazolo-quinazoline 21 worked well in this study to furnish promising IC_{50} values ranging from 8.8-15.6 μM. Furthermore, alcohol tethered benzothiazolo-quinazoline 22, derived from the reduction of the ester group of 2, provided IC_{50} values in the range of 10.1-23.6 μM. Lastly, we tested the intermediate 23, ethyl (E)-3-(2-((2-cyanamidophenyl)thio) phenyl)acrylate, to observe higher inhibitory values in the range of 9.3-12.4 μM. Thus, we show that benzothiazolo-quinazoline derivatives: 1-3, 6, 10, and 21-23 exhibited superior inhibitory effects with IC_{50} values ranging from 4.2-12.1 μM. To check that 1-3, 6, 10, and 21-23 indeed affected HeLa cell growth, we performed crystal violet staining and examined cell morphology. We found that the congeners indeed decreased crystal violet staining and altered cell morphology, indicating that the potency of the congeners (Figure 1A-B). Further, the benzothiazolo-quinazoline congeners also blocked cell migration (Figure 1C). Overall, these observations prompted us to elucidate the in-depth mechanism of action of 1-3, 6, 10, and 21-23 compounds.

Benzothiazolo-quinazoline congeners trigger G2/M arrest

The SAR analysis revealed that compounds 1-3, 6, 10, and 21-23 potently reduce the growth of cancer cells. A characteristic feature of antiproliferative compounds is that they alter cell cycle progression;[30] therefore, we asked whether these compounds also affect cell cycle progression. To answer this question, we treated HeLa cells 1-3, 6, 10, and 21-23 for 18 hr and performed cell analysis using imaging flow cytometry. As controls, we also treated HeLa cells with DMSO or nocodazole, a G2/M blocker for similar duration.[21] Here, we found that the 1-3, 6, 10, and 21-23 effectively arrested cell cycle progression in G2/M phase similar to nocodazole treatments. A representative imaging analysis also shows that benzothiazolo-quinazoline congeners treated cells have doubled DNA content compared to untreated or DMSO-treated cells (Figure 2). Thus, benzothiazolo-quinazoline congeners arrest cells in G2/M phase.

Benzothiazolo-quinazoline congeners treated cells accumulate protein and transcript levels of mitotic markers

Cyclin B1/Cdk1 and Aurora A phosphorylates mitotic proteins to ensure the orderly progression of cell division. Further, accumulation of Cyclin B1 and Aurora A is a typical feature of mitosis;[31] therefore, we checked if 1-3, 6, 10, and 21-23 affect Cyclin B1 and Aurora A protein levels. We found that the selected benzothiazolo-quinazoline congeners increase Cyclin

Table 2: Summarised *in silico* parameters of compounds, including ADMET properties.

Sl. No.	Comp	[a]DS (kcal/mol)	[b]GEM (kcal/mol)	[c]ΔGbind (kcal/mol)	ADME properties (Lipinski rule of five)						Toxicity (Protox-II server)		
					[d]MW	[e]HBD	[f]HBA	[g]cLogP	[h]TPSA	Breach of rule	[i]LD_{50} (mg/kg)	Toxicity class	Toxicity target
1	1	-7.34	-71.69	-105.00	324.403	0	4	3.168	67.2	0	600	4	None
2	2	-7.22	-66.10	-76.51	310.376	0	4	2.7617	67.2	0	700	4	None
3	3	-6.77	-68.74	-105.49	338.43	0	4	3.5119	67.2	0	700	4	None
4	6	-6.8	-65.36	-70.39	352.457	0	4	3.8558	67.2	0	2900	5	None
5	10	-7.38	-68.74	-49.52	360.383	0	4	3.3696	67.2	0	700	4	None
6	21	-7.32	-61.34	-78.38	325.391	0	5	2.5185	80.09	0	1100	4	None
7	22	-7.19	-59.26	-98.28	324.403	1	4	3.4396	87.42	0	4000	5	None
8	23	-6.74	-68.85	-71.93	282.366	1	3	2.6834	61.13	0	2900	5	None

[a]Dock score, [b]Glide Emodel, [c]MM-GBSA or binding free energy, [d]Molecular Weight, [e]H-bond donor, [f]H-bond acceptor, [g]Hydrophilicity, [h]Topological Polar Surface Area, [i]lethal dose, 50%.

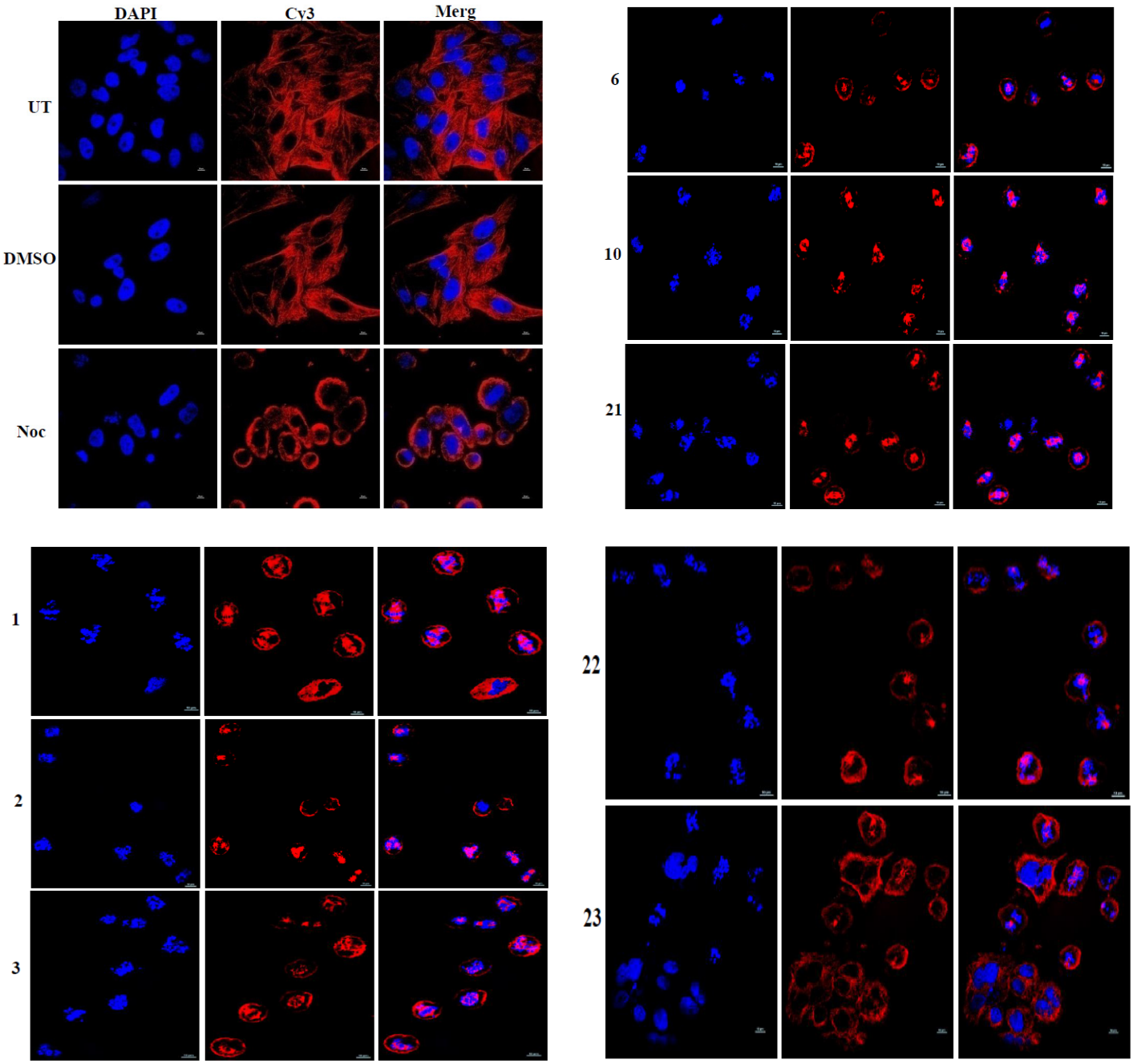

Figure 5: Benzothiazolo-quinazoline congeners disrupt microtubule network- A, HeLa cells seeded on 18 mm coverslips and were treated with 5 µM of 1-3, 6, 10, and with 10 µM 21-23 for 18 hr. Nocodazole (Noc) was used as a positive control, at 2.5 µM concentrations After 18 hr, cells were washed with 1x PBS, followed by fixation, permeabilization, and indirect immunofluorescence analysis was performed. The cells were incubated with anti-α-tubulin primary antibody and stained using Cy3-conjugated secondary antibody. Nuclei were stained with DAPI. The merged images of cells stained for tubulin and DAPI are shown. The images are representative of three independent experiments.

B1 and Aurora A protein levels similar to nocodazole (Figure 3A). To corroborate that benzothiazolo-quinazoline congeners indeed arrest cells in G2/M, we examined the transcript levels of mitotic markers including Plk1 and Nek2A in HeLa cells treated with selected congeners.[32] We observed that the selected benzothiazolo-quinazoline congeners strongly increase the transcript levels of mitotic markers similar to nocodazole-treated cells (Figure B). Overall, the compounds 1-3, 6, 10, and 21-23 increase Cyclin B1 protein and transcript levels of mitotic markers.

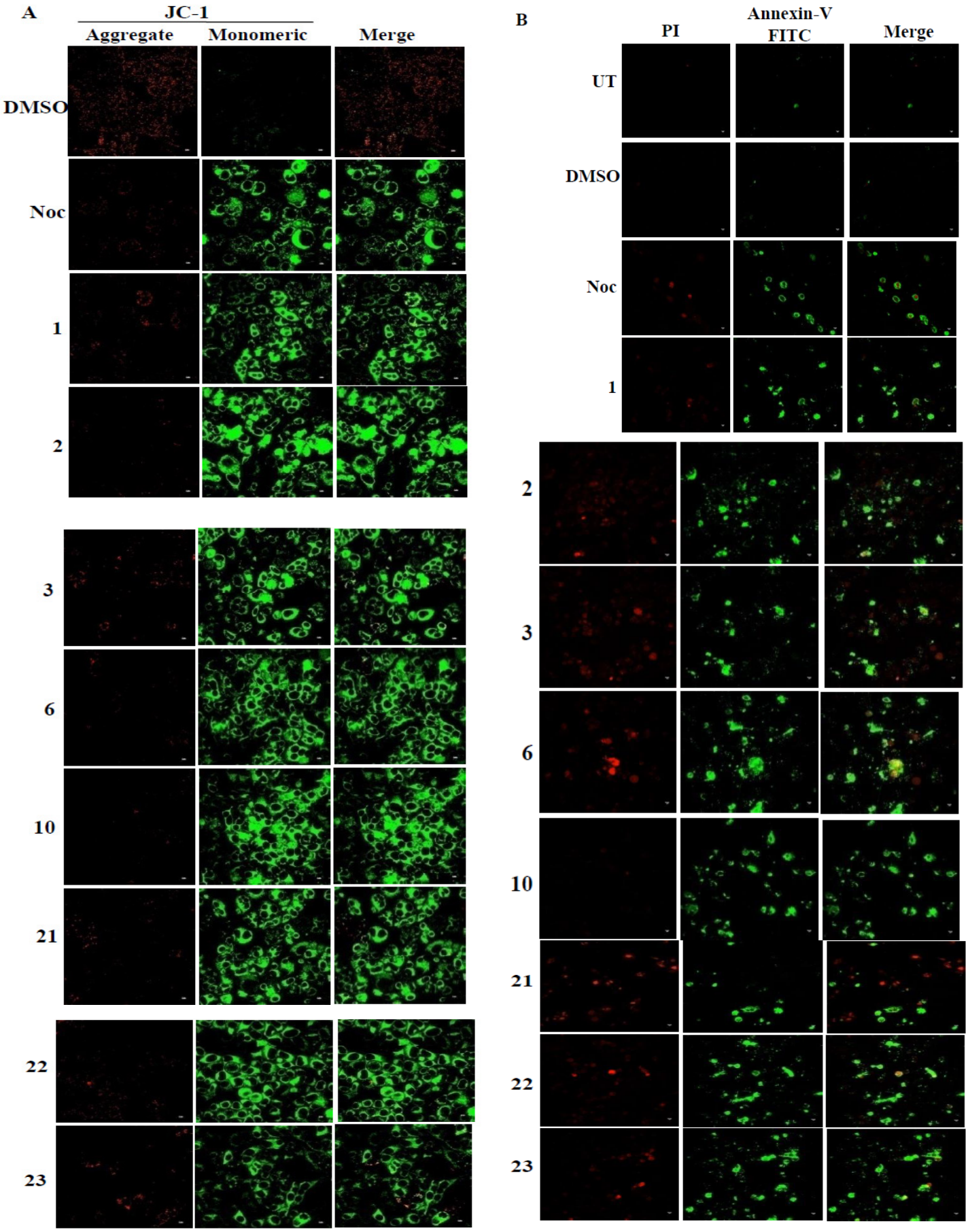
A
JC-1
Aggregate
Monomeric
Merge
DMSO
Noc
1
2
3
6
10
21
22
23
B
PI
Annexin-V
FITC
Merge
UT
DMSO
Noc
1
2
3
6
10
21
22
23

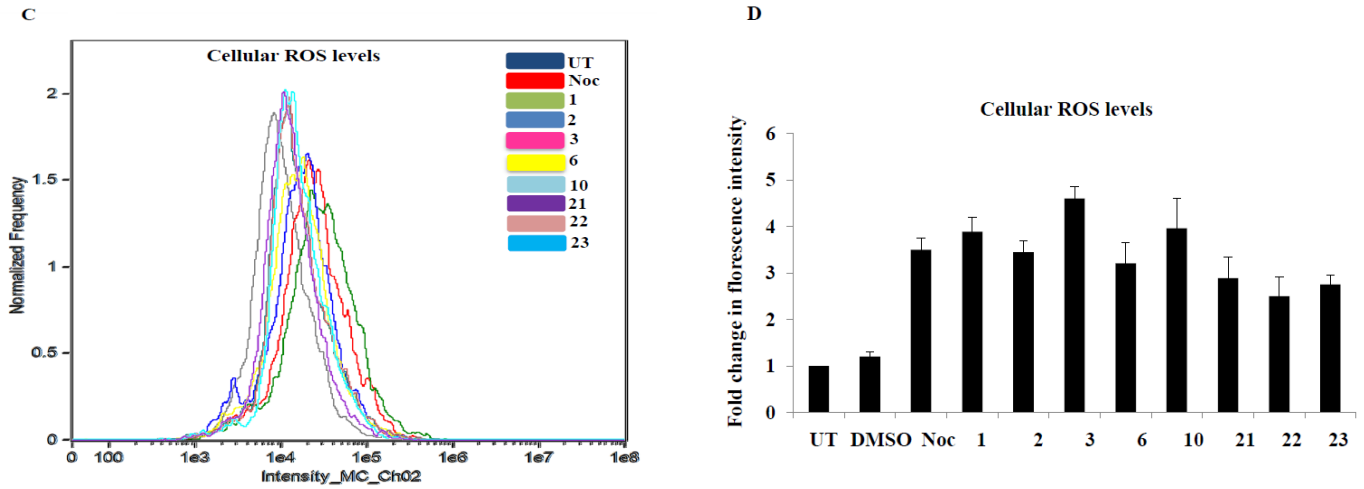

Figure 6: Benzothiazolo-quinazoline congeners increase mitochondrial depolarization, induce Annexin V, and activate cellular reactive oxygen species (ROS) levels and staining A, HeLa cells seeded on 18 mm coverslips and were treated with 5 µM of 1-3, 6, 10, and with 10 µM 21-23 for 18 hr. Nocodazole (Noc) was used as a positive control, at 2.5 µM concentrations. After 18 hr, the cells were treated with JC-1 and confocal microscopy was performed to determine mitochondrial polarization. Depolarized mitochondria emit green fluorescence and polarized mitochondria emit red fluorescence. PI represents Propidium iodide. Representative images from three independent experiments are shown *n*=3. B, under similar treatment conditions of A, apoptosis was assessed using the ApoAlert Annexin V Apoptosis Detection Kit, Clontech according to the manufacturer's instructions. Representative images from three independent experiments are shown *n*=3. C-D, under similar treatment conditions of A, after treatments, the cells were centrifuged at 1000 rpm for 1 min. The centrifuged cells were washed using 1 x PBS and incubated with 20 µM DCF-DA for 20 min at 370C in a CO_2 incubator. The incubated cells were washed with 1x PBS and fluorescence intensity was measured at λ_{ex}=485 nm/λ_{em}=520 nm in an Amnis Flowsight Flow cytometer and the mean fluorescence intensity was calculated. C is a representative image of ROS intensity calculated using flow cytometry, and D, is the graph plotted as fold change of fluorescence intensity.

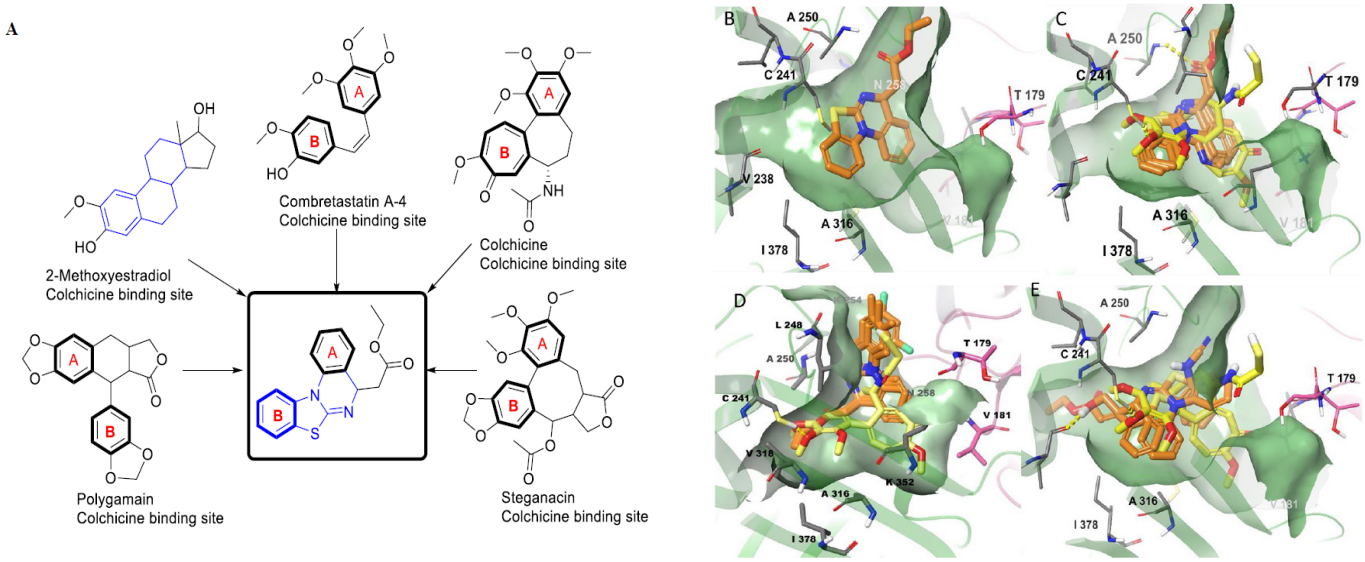

Figure 7: Benzothiazolo-quinazoline congeners occupy the colchicine binding site of tubulin. A, Structural similarities of compound 1 with other prominent colchicine binding agents. B, compound 1 in colchicine binding pocket. C, series-1 overlap with colchicine. D, series-2 overlap with colchicine. E, compound 22 and 23 overlap with colchicine. Here, yellow sticks represent Colchicine, orange sticks represent ligands, the β-tubulin residues are represented by grey thin sticks, and α-tubulin residues are pink thin sticks.

Benzothiazolo-quinazoline congeners act as microtubule depolymerising agents

As the selected congener's phenocopy nocodazole, a microtubule depolymerising agent by arresting cells in G2/M and increasing mitotic markers, so we checked whether the benzothiazolo-quinazoline congeners show similar mechanism of action. To check, we treated HeLa cells with 1-3, 6, 10, and 21-23 for 18 hr and then collected soluble and insoluble fractions for immunoblot analysis. As controls, we also treated HeLa cells with DMSO, nocodazole, or paclitaxel, a microtubule polymerising agent for similar duration. We observed that the selected benzothiazolo-quinazoline congeners have more soluble tubulin levels similar to nocodazole. In comparison, DMSO-treated cells had fairly equal levels of tubulin indicating homeostasis, whereas Paclitaxel-treated cells had more insoluble tubulin levels (Figure

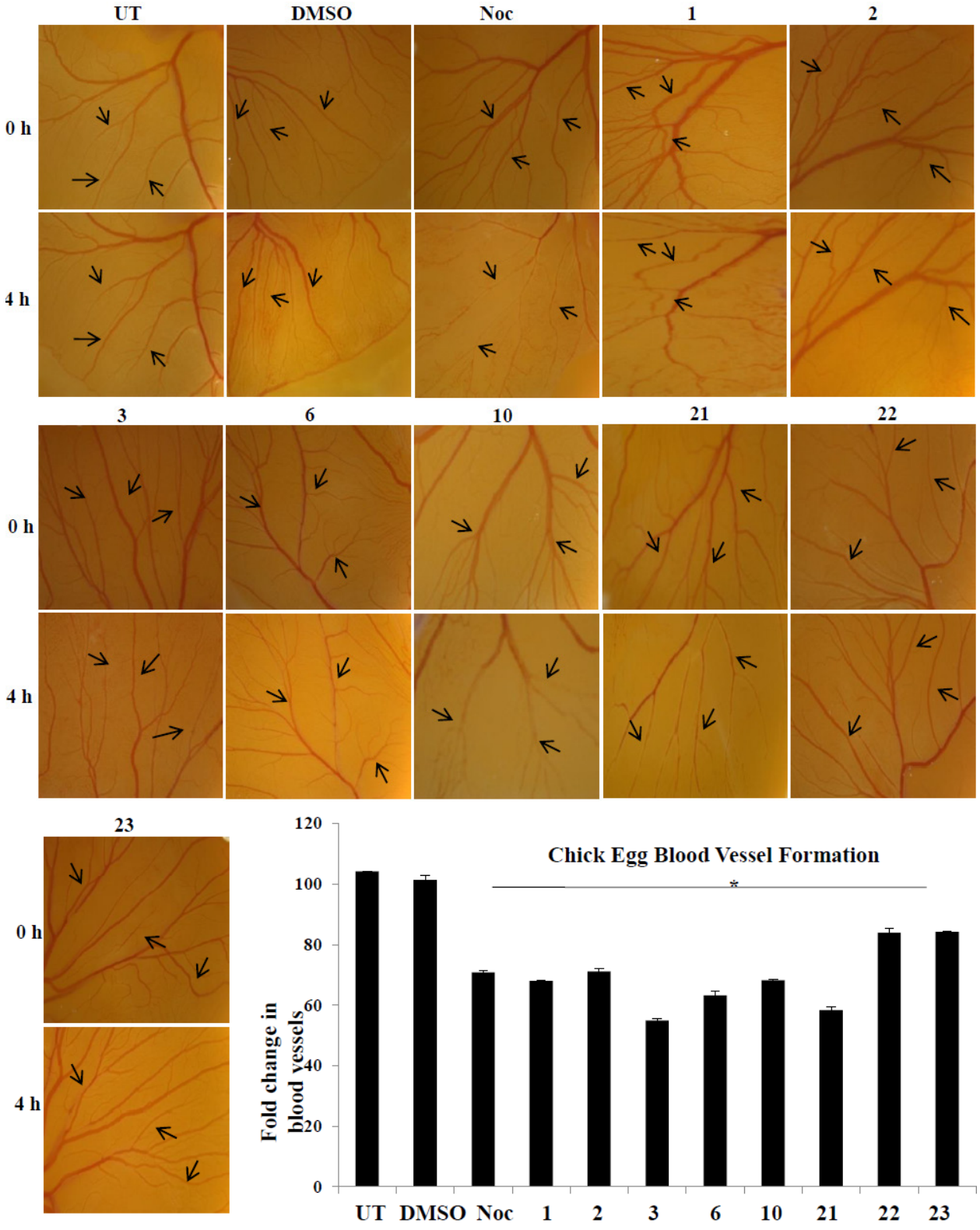

Figure 8: Benzothiazolo-quinazoline congeners block angiogenesis in chick embryos- Chick embryos were treated with 5 µM of 1-3, 6, 10, and with 10 µM 21-23 at 0 hr and 4 hr. Nocodazole (Noc) was used as a positive control, at 2.5 µM concentrations. Images were quantified using Image J software. and plotted as fold change in blood vessel formation and represented as mean±SD. Significant differences from UT embryo were observed (*p<0.05), n=3.

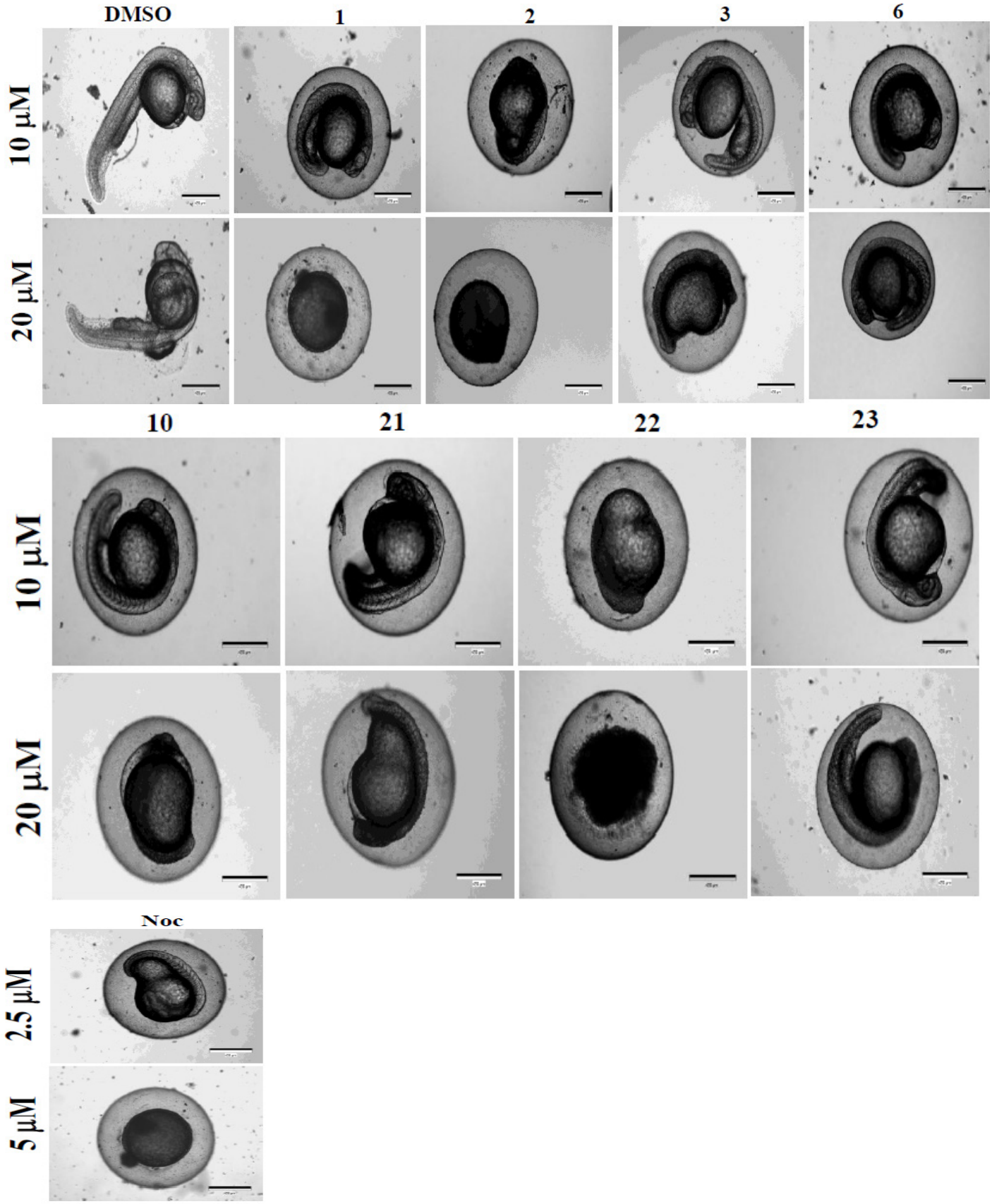

Figure 9: Benzothiazolo-quinazoline congeners inhibit zebrafish embryo growth-Zebrafish embryos were treated with 10 µM and 20 µM of 1-3, 6, 10, 21-23 at 5 hr post fertilization. Nocodazole (Noc) was used as a positive control, at 2.5 µM and 5 µM concentrations After 28 hr, the embryos were imaged using microscopy to observe morphological changes.

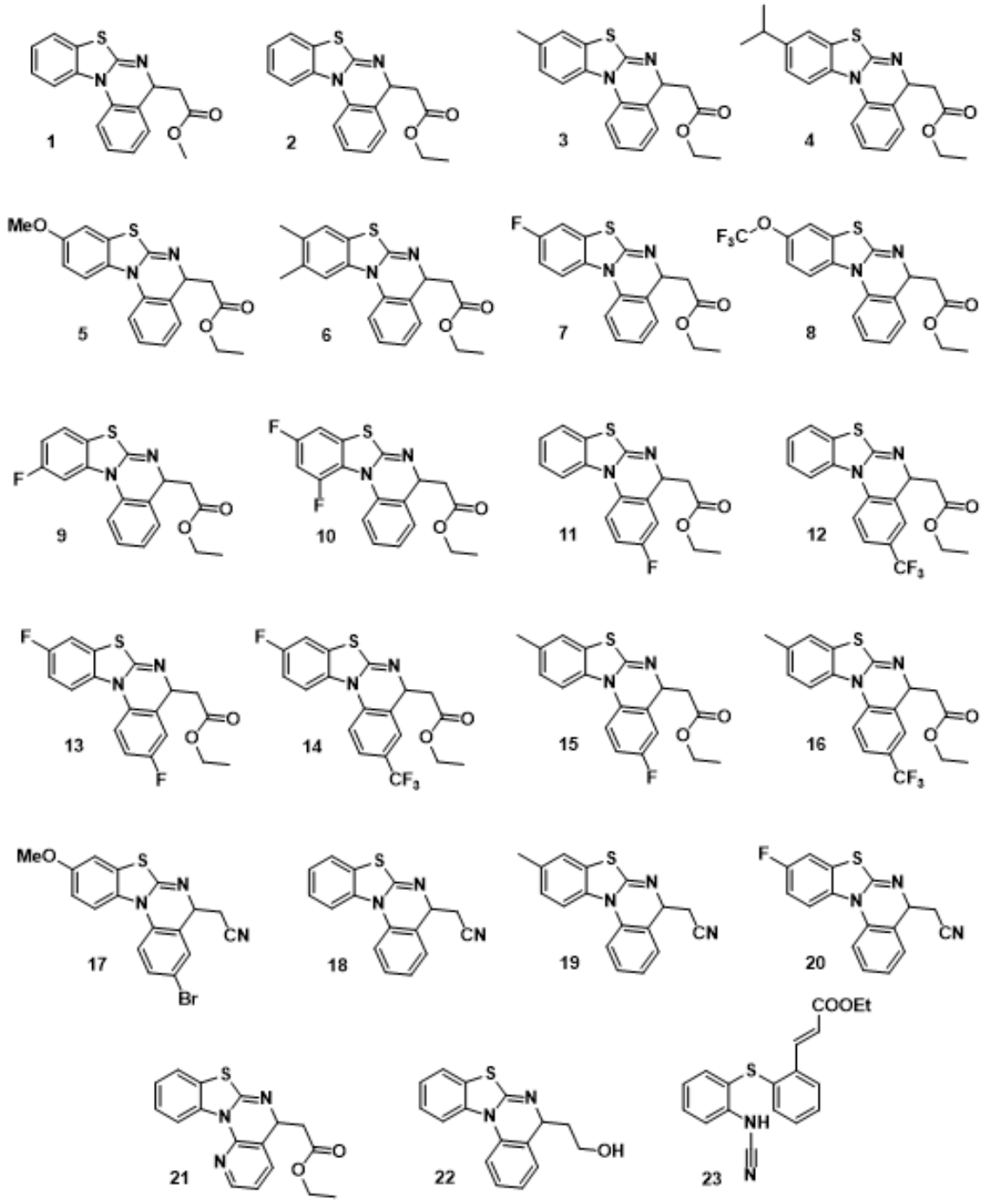

Chart 1: Benzothiazolo-quinazoline congeners, 1-23 were employed in the study.

4). Taken together, the benzothiazolo-quinazoline congeners act microtubule depolymerising agents by increasing soluble tubulin levels.

Benzothiazolo-quinazoline congeners disrupt microtubule network

Microtubule network is disrupted during cell division, where in microtubules bind to and aid in the separation of chromosomes. As benzothiazolo-quinazoline congeners arrest cells in G2/M and increase mitotic markers, we checked if the benzothiazolo-quinazoline affects cellular phenotype. To check, we treated HeLa cells with the selected benzothiazolo-quinazoline congeners for 18 hr and stained for tubulin protein. Immunofluorescence analysis revealed that HeLa cells treated with selected benzothiazolo-quinazoline congeners have spindle microtubules with centrally located chromosome (Figure

5). Taken together, the selected benzothiazolo-quinazoline derivatives trigger a change in HeLa cells from a normal phenotype to mitosis.

Benzothiazolo-quinazoline congeners depolarise mitochondria, induce ROS and promote mitotic cell death

Anticancer agents deplete cellular glutathione levels and increase ROS levels to trigger ROS-dependent cell death.[33] As benzothiazolo-quinazoline congeners 1-3, 6, 10, and 21-23 reduce cell growth and arrest cells in G2/M; thus, we determined if benzothiazolo-quinazoline congeners depolarise mitochondria and activate cell death. For mitochondria, we performed JC-1 staining, and found that benzothiazolo-quinazoline congener treated cells harboured depolarised mitochondria, as evidenced by strong JC-1 aggregate staining (Figure 6A). For cell death, we treated HeLa cells with compounds and examined for Annexin-V staining. We found that benzothiazolo-quinazoline congeners activate mitotic cell death as evidenced by strong Annexin-V staining (Figure 6B). Next, we checked for another apoptotic parameter, cellular Reactive Oxygen Species (ROS) levels; we treated HeLa cells with selected congeners and performed cytometry analysis. We found that selected congeners increase cellular ROS levels, suggesting that the congeners trigger ROS-dependent cell death (Figure 6C). Taken together, the benzothiazolo-quinazoline congeners depolarise mitochondria, induce ROS and promote mitotic cell death in HeLa cells.

Benzothiazolo-quinazoline congeners occupy the colchicines binding site of tubulin

Colchicine is a natural product binding at the interface of α and β subunits in the Colchicine Binding Pocket (CBP) that binds tubulin and inhibits tubulin polymerisation. The CBP is constructed by the strands S8 and S9, loop T7, and helices H7 and H8; the pocket is divided into three zones (zone-1 to 3). The peripheral residues of α and β tubulins form zone-1, zone-2, and zone-3 are situated in β-tubulin, where zone-2 forms the main pocket and zone-3 extends further into the β-tubulin forming an extended pocket.[34-36] The colchicine binds in the main cavity (zone-2) and extends into zone-1. The ring-A methoxy groups interacts with βC241 and the ring-B associate with αT179, and αV181 residues.[37,38] The docking of these compounds obtained good binding modes (~-7.0 kcal/mol) (Table 2) and interaction analysis revealed three different binding patterns. The set-1 compounds (1, 2, and 21) occupied zone-2 of CBP similar to colchicine in set-1 compounds, three rings (quinazoline and thiazole) were homologus to three rings of colchicine and the remaining fourth ring occupied the cavity designated for methoxy groups. The most active compound 1 exhibited a dock score of -7.34 kcal/mol and has a high Glide Emodel value of -71.69 kcal/mol, along with increase in binding free energy ($\Delta G_{bind=}$-105.00 kcal/mol), showing good affinity and excellent occupancy (Figure 7B). We found that the ester tail extended into zone-1 similar to the amide residue of colchicine (Figure 7C). Further, we observed that 2 has a good dock score (-7.22 kcal/mol), binding free energy (-76.51 kcal/mol), and Emodel score (-66.10 kcal/mol), and the ester carbonyl of 2 formed an H-bond with βA250 (backbone), possibly contributing to better cytotoxicity. Finally, 21 also displayed good affinity (-7.32 kcal/mol), though relatively less cytotoxic. The set-2 (3, 6, and 10) on the other hand, displayed an inverted mode of binding where the aromatic rings occupied the sidechain region of colchicine while extending the ester tail into zone-2 (Figure 7D). Furthermore, diflouro substituted aromatic ring (ring-B) of 10 also formed π-cation interaction with βK254 (side chain), which might have contributed to its high binding efficiency (-7.38 kcal/mol). Nevertheless, its poor binding free energy (-49.52 kcal/mol) indicates forced binding. Interestingly, set-1 seems to have more affinity towards tubulin binding, which is clearly depicted by excellent binding efficiencies (Table 2). Compound 22 occupied zone-2 and the alcohol sidechain slightly extended into zone-3, towards the methoxy region of colchicine with a moderate binding (-6.74 kcal/mol); similarly, 23 also extends into zone-3 (Figure 7E). The polar nature of these sidechains might cause the decrease in cytotoxicity as the polar 22 is relatively less active, coinciding with the decrease in dock score. The (*S*)-enantiomer of the ligands showed preferable affinity towards tubulin compared to their counterparts. The ADME study identified the ligands as drug like that obeyed Lipinski rule of five. Additionally, the toxicity prediction from ProTox-II established their non-toxic nature. The Table 2 summarised all the *in silico* parameters and docking parameters of the compounds, respectively.

Benzothiazolo-quinazoline congeners block angiogenesis in chick embryos

Anti-microtubule agents such as combretastatins, BNC105, colchicines, and phenylahistin were shown to occupy the colchicine site in the microtubule and disrupt blood vessel formation in tumors. These set of compounds were classified as vascular disrupting agents.[39,40] As benzothiazolo-quinazoline congeners 1-3, 6, 10, and 21-23 also disrupt tubulin polymerization and occupy colchicine site, therefore, we asked whether benzothiazolo-quinazoline congeners can function as vascular disrupting agents. To answer this question, we performed the chick embryo angiogenesis assays and examined the formation of the blood vasculature. We found that the selected benzothiazolo-quinazoline congeners effectively disrupt blood vasculature, but not in DMSO-treated eggs (Figure 8). Finally, these results show that benzothiazolo-quinazoline congeners can be employed as vascular disrupting agents.

Benzothiazolo-quinazoline congeners inhibit zebrafish embryo growth

Zebrafish (*Danio rerio*) is an emerging model system to elucidate chemical genetics.[41] To check whether benzothiazolo-quinazoline congeners can affect zebrafish embryos development, we treated embryos with benzothiazolo-quinazoline congeners 1-3, 6, 10, and 21-23 and examined the treated embryos. We found that benzothiazolo-quinazoline congeners delayed embryo development when compared to DMSO-treated or control embryos. The control embryos traversed to the prim6 stage, whereas the benzothiazolo-quinazoline congener's embryos were arrested at the 18-cell somite stage. As a control, we found that nocodazole-treated embryos also show similar abnormalities in development (Figure 9). Based on these observations, we show that benzothiazolo-quinazoline congeners can function as potential chemotherapeutic leads.

CONCLUSION

In the present study, we show that that eight benzothiazolo-uinazoline congeners act as anti-microtubule agents. The congeners are amenable for further structural modifications and can be lead-optimised into next generation anti-microtubule agents.

ACKNOWLEDGEMENT

This work was supported by grant from Indian Council of Medical Research, GAP-0987 to N.J. S.B acknowledges Department of Biochemistry, Osmania University and Director IICT for PhD registration and SS thanks UGC for the SRF fellowship. The authors thank Zebrafish facility of CSIR-IICT, Dr. Sumana Chakravarty, and Chinmayee Tripathy for assistance. SB thanks Dr. Chittaranjan Patra and Proma Nag Chowdhury for assistance in performing angiogenesis assays. The authors thank Director CSIR-IICT for providing research facilities (IICT/Pubs./2023/277).

FUNDING

From Indian Council of Medical Research, GAP-0987

CONFLICT OF INTEREST

The authors declare that there is no conflict of interest.

ABBREVIATIONS

DMEM: Dulbecco's modified Eagle's medium; **ROS:** Reactive oxygen species; **SDS-PAGE:** Sodium dodecyl sulfate-polyacrylamide gel electrophoresis; **PBS:** Phosphate buffer saline; **ECL:** Enhanced chemiluminescence; **Noc:** Nocodazole; **ATCC:** American Type Culture Collection.

AUTHORS' CONTRIBUTION

Supriya Bhukya: Conceptualization, Methodology, Validation, Data curation, Writing-original draft, Writing-review and editing, Sonam Swain, Darna Mounika Methodology, Validation, Data curation. Jyoti Honnanayakanavar, Battu Harish, Purna Chandra Behera, Validation, Data curation. Vidya Jyothi Alli, Methodology, Validation Supervision, Surender Singh Jadav, Writing-review and editing, Investigation, Methodology, Validation, Data Anthony Addlagatta, Surisetti Suresh, Nishant Jain, Writing-original draft, Writing-review and editing, Conceptualization, Investigation, Project administration, Funding acquisition.

REFERENCES

1. Hoelder S, Clarke PA, Workman P. Discovery of small molecule cancer drugs: successes, challenges and opportunities. Mol Oncol. 2012;6(2):155-76. doi: 10.1016/j.molonc.2012.02.004, PMID 22440008.
2. Tsimberidou AM, Fountzilas E, Nikanjam M, Kurzrock R. Review of precision cancer medicine: evolution of the treatment paradigm. Cancer Treat Rev. 2020;86:102019. doi: 10.1016/j.ctrv.2020.102019, PMID 32251926.
3. Anand U, Dey A, Chandel AKS, Sanyal R, Mishra A, Pandey DK, *et al*. Cancer chemotherapy and beyond: current status, drug candidates, associated risks and progress in targeted therapeutics. Genes Dis. 2023;10(4): 1367-401. doi: 10.1016/j.gendis.2022.02.007, PMID 37397557.
4. Shah SC, Kayamba V, Peek RM, Heimburger D. Cancer control in low- and middle-income countries: is it time to consider screening? J Glob Oncol. 2019;5(5):1-8. doi: 10.1200/JGO.18.00200, PMID 30908147.
5. Kasztura M, Richard A, Bempong NE, Loncar D, Flahault A. Cost-effectiveness of precision medicine: a scoping review. Int J Public Health. 2019;64(9):1261-71. doi: 10.1007/s00038-019-01298-x, PMID 31650223.
6. Gallego-Jara J, Lozano-Terol G, Sola-Martínez RA, Cánovas-Díaz M, de Diego Puente T. A compressive review about Taxol®: history and future challenges. Molecules. 2020;25(24):5986. doi: 10.3390/molecules25245986, PMID 33348838.
7. Brouhard GJ, Rice LM. Microtubule dynamics: an interplay of biochemistry and mechanics. Nat Rev Mol Cell Biol. 2018;19(7):451-63. doi: 10.1038/s41580-018-0009-y, PMID 29674711.
8. Vitale I, Galluzzi L, Castedo M, Kroemer G. Mitotic catastrophe: a mechanism for avoiding genomic instability. Nat Rev Mol Cell Biol. 2011;12(6):385-92. doi: 10.1038/nrm3115, PMID 21527953.
9. Klein I, Lehmann HC. Pathomechanisms of paclitaxel-induced peripheral neuropathy. Toxics. 2021;9(10):229. doi: 10.3390/toxics9100229, PMID 34678925.
10. Chen YF, Wu CH, Chen LH, Lee HW, Lee JC, Yeh TK, *et al.* Discovery of potential neuroprotective agents against paclitaxel-induced peripheral neuropathy. J Med Chem. 2022;65(6):4767-82. doi: 10.1021/acs.jmedchem.1c01912, PMID 35234475.
11. Honnanayakanavar JM, Harish B, Nanubolu JB, Suresh S. Tandem copper-catalyzed regioselective N-Arylation-Aza-Michael addition: synthesis of tetracyclic 5H-Benzothiazolo[3,2-a]quinazoline derivatives. J Org Chem. 2020;85(14):8780-91. doi: 10.1021/acs.joc.0c00275, PMID 32603597.
12. Welsch ME, Snyder SA, Stockwell BR. Privileged scaffolds for library design and drug discovery. Curr Opin Chem Biol. 2010;14(3):347-61. doi: 10.1016/j.cbpa.2010.02.018, PMID 20303320.
13. Rouf A, Tanyeli C. Bioactive thiazole and benzothiazole derivatives. Eur J Med Chem. 2015;97:911-27. doi: 10.1016/j.ejmech.2014.10.058, PMID 25455640.
14. Gerna G, Lilleri D, Baldanti F. An overview of letermovir: a cytomegalovirus prophylactic option. Expert Opin Pharmacother. 2019;20(12):1429-38. doi: 10.1080/14656566.2019.1637418, PMID 31282759.
15. Sanford M, Scott LJ. Gefitinib: a review of its use in the treatment of locally advanced/metastatic non-small cell lung cancer. Drugs. 2009;69(16):2303-28. doi: 10.2165/10489100-000000000-00000, PMID 19852530.
16. Shukla G, Tiwari AK, Singh VK, Bajpai A, Chandra H, Mishra AK. Effect of a novel series of Benzothiazolo-Quinazolones on epidermal growth factor receptor (EGFR) and biological evaluations. Chem Biol Drug Des. 2008;72(6):533-9. doi: 10.1111/j.1747-0285.2008.00724.x, PMID 19090920.
17. Khalilzadeh MA, Karimi-Maleh H, Gupta VK. A nanostructure based electrochemical sensor for square wave voltammetric determination of L-cysteine in the presence of high concentration of folic acid. Electroanalysis. 2015;27(7):1766-73. doi: 10.1002/elan.201500040.
18. Karimi-Maleh H, Tahernejad-Javazmi F, Gupta VK, Ahmar H, Asadi MH. A novel biosensor for liquid phase determination of glutathione and amoxicillin in biological and pharmaceutical samples using a ZnO/CNTs nanocomposite/catechol derivative modified electrode. J Mol Liq. 2014;196:258-63. doi: 10.1016/j.molliq.2014.03.049.

19. LoRusso PM, Gadgeel SM, Wozniak A, Barge AJ, Jones HK, DelProposto ZS, *et al*. Phase I clinical evaluation of ZD6126, a novel vascular-targeting agent, in patients with solid tumors. Investig New Drugs. 2008;26(2):159-67. doi: 10.1007/s10637-008-9112-9, PMID 18219445.
20. Reddy MA, Jain N, Yada D, Kishore C, Vangala JR, P Surendra R, *et al*. Design and synthesis of resveratrol-based Nitrovinylstilbenes as antimitotic agents. J Med Chem. 2011;54(19):6751-60. doi: 10.1021/jm200639r, PMID 21851083.
21. Pamarthy D, Behera SK, Swain S, Yadav S, Suresh S, Jain N, *et al.* Diaryl ether derivative inhibits GPX4 expression levels to induce ferroptosis in thyroid cancer cells. Drug Dev Res. 2023;84(5):861-87. doi: 10.1002/ddr.22059, PMID 37070554.
22. Lambhate S, Bhattacharjee D, Jain N. APC/C CDH1 ubiquitinates IDH2 contributing to ROS increase in mitosis. Cell Signal. 2021;86:110087. doi: 10.1016/j.cellsig.2021.110087, PMID 34271087.
23. Bhattacharjee D, Balabhaskararao K, Jain N. Mutant IDH1 inhibitors activate pSTAT3-Y705 leading to an increase in BCAT1 and YKL-40 levels in mutant IDH1-expressing cells. Biochim Biophys Acta Mol Cell Res. 2021;1868(11):119114. doi: 10.1016/j.bbamcr.2021.119114, PMID 34329662.
24. Poornima B, Siva B, Venkanna A, Shankaraiah G, Jain N, Yadav DK, *et al*. Novel Gomisin B analogues as potential cytotoxic agents: design, synthesis, biological evaluation and docking studies. Eur J Med Chem. 2017;139:441-53. doi: 10.1016/j.ejmech.2017.07.076, PMID 28818768.
25. Bhattacharjee D, Kaveti S, Jain N. APC/C CDH1 ubiquitinates STAT3 in mitosis. Int J Biochem Cell Biol. 2023;154:106333. doi: 10.1016/j.biocel.2022.106333, PMID 36400381.
26. Bala Bhaskara Rao KB, Katragunta K, Sarma UM, Jain N. Abundance of d-2-hydroxyglutarate in G2/M is determined by FOXM1 in mutant IDH1-expressing cells. FEBS Lett. 2019;593(16):2177-93. doi: 10.1002/1873-3468.13500, PMID 31211872.
27. Bhattacharjee D, Bakar J, Chitnis SP, Sausville EL, Ashtekar KD, Mendelson BE, *et al*. Inhibition of a lower potency target drives the anticancer activity of a clinical p38 inhibitor. Cell Chem Biol. 2023;30(10):1211-1222.e5. doi: 10.1016/j.chembiol.2023.09.013, PMID 37827156.
28. Banerjee P, Eckert AO, Schrey AK, Preissner R. ProTox-II: a webserver for the prediction of toxicity of chemicals. Nucleic Acids Res. 2018;46(W1):W257-63. doi: 10.1093/nar/gky318, PMID 29718510.
29. Sander T, Freyss J, von Korff M, Rufener C. DataWarrior: an open-source program for chemistry aware data visualization and analysis. J Chem Inf Model. 2015;55(2):460-73. doi: 10.1021/ci500588j, PMID 25558886.
30. Mukherjee S, Kotcherlakota R, Haque S, Bhattacharya D, Kumar JM, Chakravarty S, *et al*. Improved delivery of doxorubicin using rationally designed pegylated platinum nanoparticles for the treatment of melanoma. Mater Sci Eng C Mater Biol Appl. 2020;108:110375. doi: 10.1016/j.msec.2019.110375, PMID 31924026.
31. Das S, Roy A, Barui AK, Alabbasi MMA, Kuncha M, Sistla R, *et al*. Anti-angiogenic vanadium pentoxide nanoparticles for the treatment of melanoma and their *in vivo* toxicity study. Nanoscale. 2020;12(14):7604-21. doi: 10.1039/d0nr00631a, PMID 32232245.
32. Kamal A, Shaik AB, Polepalli S, Reddy VS, Kumar GB, Gupta S, *et al*. Pyrazole-oxadiazole conjugates: synthesis, antiproliferative activity and inhibition of tubulin polymerization. Org Biomol Chem. 2014;12(40):7993-8007. doi: 10.1039/c4ob01152j, PMID 25181296.
33. Kamal A, Shaik AB, Jain N, Kishor C, Nagabhushana A, Supriya B, *et al*. Design and synthesis of pyrazole-oxindole conjugates targeting tubulin polymerization as new anticancer agents. Eur J Med Chem. 2015;92:501-13. doi: 10.1016/j.ejmech.2013.10.077, PMID 25599948.
34. Bai J, Li Y, Zhang G. Cell cycle regulation and anticancer drug discovery. Cancer Biol Med. 2017;14(4):348-62. doi: 10.20892/j.issn.2095-3941.2017.0033, PMID 29372101.
35. Gavet O, Pines J. Progressive activation of CyclinB1-Cdk1 coordinates entry to mitosis. Dev Cell. 2010;18(4):533-43. doi: 10.1016/j.devcel.2010.02.013, PMID 20412769.
36. Alexander J, Lim D, Joughin BA, Hegemann B, Hutchins JRA, Ehrenberger T, *et al*. Spatial exclusivity combined with positive and negative selection of phosphorylation motifs is the basis for context-dependent mitotic signaling. Sci Signal. 2011;4(179):ra42-. doi: 10.1126/scisignal.2001796, PMID 21712545.
37. Redza-Dutordoir M, Averill-Bates DA. Activation of apoptosis signalling pathways by reactive oxygen species. Biochim Biophys Acta. 2016;1863(12):2977-92. doi: 10.1016/j.bbamcr.2016.09.012, PMID 27646922.
38. Ravelli RBG, Gigant B, Curmi PA, Jourdain I, Lachkar S, Sobel A, *et al*. Insight into tubulin regulation from a complex with colchicine and a stathmin-like domain. Nature. 2004;428(6979):198-202. doi: 10.1038/nature02393, PMID 15014504.
39. Dorléans A, Gigant B, Ravelli RBG, Mailliet P, Mikol V, Knossow M. Variations in the colchicine-binding domain provide insight into the structural switch of tubulin. Proc Natl Acad Sci U S A. 2009;106(33):13775-9. doi: 10.1073/pnas.0904223106, PMID 19666559.
40. Wang J, Miller DD, Li W. Molecular interactions at the colchicine binding site in tubulin: an X-ray crystallography perspective. Drug Discov Today. 2022;27(3):759-76. doi: 10.1016/j.drudis.2021.12.001, PMID 34890803.
41. Naaz F, Haider MR, Shafi S, Yar MS. Anti-tubulin agents of natural origin: targeting Taxol, vinca, and colchicine binding domains. Eur J Med Chem. 2019;171:310-31. doi: 10.1016/j.ejmech.2019.03.025, PMID 30953881.

Cite this article: Bhukya S, Swain S, Mounika D, Honnanayakanavar J, Harish B, Behera PC, *et al*. Benzothiazolo-quinazoline Congeners Function as Anti-microtubule Agents Triggering Mitotic Arrest in Cancer Cells. Int. J. Pharm. Investigation. 2024;14(2):436-53.